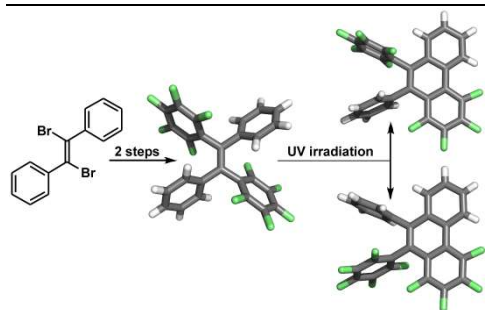


# Synthesis and Photocyclization of Fluorinated Tetraphenylethylenes

Zhenglin Zhang, Thien Lieu, Xiqu Wang, Olafs Daugulis\* and Ognjen Š. Miljanić\*

Department of Chemistry, University of Houston, 3585 Cullen Boulevard #112, Houston, TX 77204-5003, USA.

Supporting Information Placeholder



**ABSTRACT:** Five extensively fluorinated tetraphenylethylene (TPE) derivatives have been synthesized using combinations of Cu-catalyzed C–H functionalization reactions and Stille couplings. Surprisingly, in contrast to the parent TPE, these compounds show little to no aggregation-induced emission (AIE). Instead, photocyclization into fluorinated phenanthrene products occurs. Effects of solvent and oxygen on the yield and selectivity of this photocyclization have been examined.

Tetraphenylethylene (**1**, TPE) is a classic example of a molecule exhibiting aggregation-induced emission (AIE)<sup>1</sup> and has been widely used to develop responsive fluorescent materials in physical, chemical, and biological settings.<sup>2</sup> Fluorination of functional organic molecules and materials has often been used to modulate their physical and chemical characteristics.<sup>3</sup> Partial fluorination of the TPE structural motif was reported to increase the fluorescence quantum yields in crystals<sup>4a,b</sup> in addition to simplifying the separation of isomers on account of strong dipole-dipole intermolecular interactions.<sup>4c</sup> Our work on fluorinated aromatic pyrazoles<sup>5</sup> suggested that the intra- and intermolecular interactions of fluorinated aromatic rings influence the molecules' AIE activity<sup>6</sup> and allow emission color switching in aggregates and the solid state.<sup>7</sup> The fluorinated TPEs studied thus far have been ornamented with one, two, or three fluorine atoms on their aromatic rings, and they maintained AIE behavior. In this Letter, we report the synthesis and extensive characterization of four new, more extensively fluorinated tetraphenylethylene derivatives **2**, **3a**, **3b**, and **3c** (Scheme 1), as well as a triarylated ethylene **4**. We also report on the investigation of their crystal structures and optical properties, as well as their photochemical cyclization.

Syntheses of **2–4** commenced with the known dibrominated precursors **A–D**.<sup>8</sup> The introduction of the first pentafluorophenyl group was achieved by the direct C–H functionalization of pentafluorobenzene under Cu-catalyzed conditions (Scheme 1). Re-

placement of the second bromine atom required the use of Stille coupling with either PhSnBu<sub>3</sub> in the case of **2**, or C<sub>6</sub>F<sub>5</sub>SnBu<sub>3</sub> in the case of **3a–c** and **4**. The two-step sequences provided compound **2** with a single fluorinated ring, and compound **3a–3c** with two fluorinated rings in three isomeric arrangements. Our attempts to produce the perfluorinated derivative of **1** failed, as one of the bromine atoms in **D** got reductively replaced with hydrogen—leading instead to the extensively fluorinated triarylated alkene **4**. Compounds **2–4** were obtained in moderate overall yields ranging from 23 to 49%,<sup>9</sup> and were characterized by <sup>1</sup>H, <sup>19</sup>F, and <sup>13</sup>C NMR spectroscopy, FT-IR spectroscopy, mass spectrometry, and elementary analysis (details provided in the SI).

Diffraction-quality single crystals of compounds **3b**, **3c**, and **4** were obtained by slow evaporation of their solutions (1 mg mL<sup>-1</sup>) in MeOH; a preliminary crystal structure of **3a** was also obtained, but the data was of insufficient quality to allow full refinement. Crystal structures of **3a–c** and **4** are shown in Figure 1. Noticeable is the significant twisting of aromatic rings in all four systems. This deplanarization effectively prevents face-to-face [π...π] stacking despite the presence of electronically complementary fluorinated and non-fluorinated aromatic motifs.

The prepared crystals of fluorinated compounds show solid-state fluorescence (Figure S40), with emission maxima at 450 (for compound **2**), 449 (**3a**), 428 (**3b**), 521 (**3c**), and 416 (**4**) nm. The blue shift of the emission maximum from **1** (452 nm) to **3b** (428 nm) to

**4** (416 nm) can be rationalized by the increasing HOMO–LUMO gaps, which were calculated to be 95.6 kcal mol<sup>-1</sup> for **1**,<sup>10</sup> 103.4 kcal mol<sup>-1</sup> for **3b**, and 113.3 kcal mol<sup>-1</sup> for **4**. The calculated HOMO–LUMO gap of **3a** (104.8 kcal mol<sup>-1</sup>) is higher than in **3b**, but **3a** has a solid-state emission peak at a longer wavelength (449 nm) than **3b** (428 nm), implying intermolecular conjugation in the crystal of **3a**. This viewpoint is tentatively supported by **3a**'s preliminary crystal structure, which shows intermolecular slipped [ $\pi\cdots\pi$ ] stacking (Figure S38). The HOMO–LUMO energy gap of **3c** (108.2 kcal mol<sup>-1</sup>) is higher than those of **3a** and **3b** but shows a bathochromically shifted solid-state emission maximum at 521 nm, which is also due to slipped intermolecular [ $\pi\cdots\pi$ ] stacking (Figure S39).

**Scheme 1.** Syntheses of fluorinated TPE derivatives **2** and **3a–c**, and compound **4**.

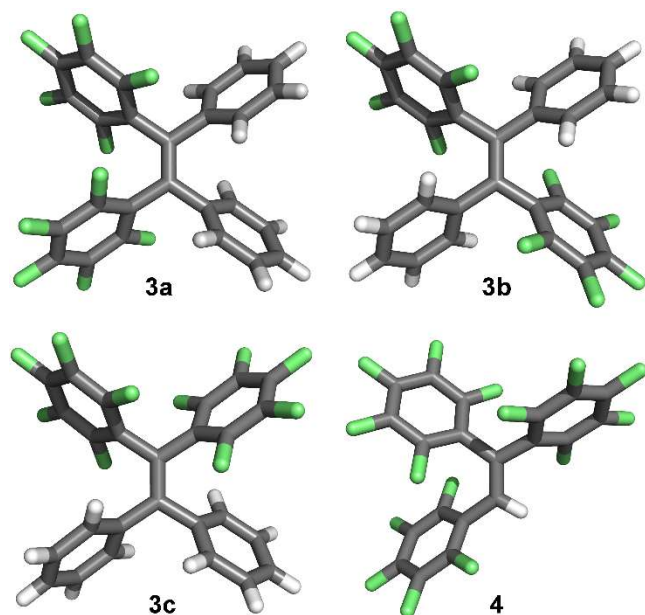
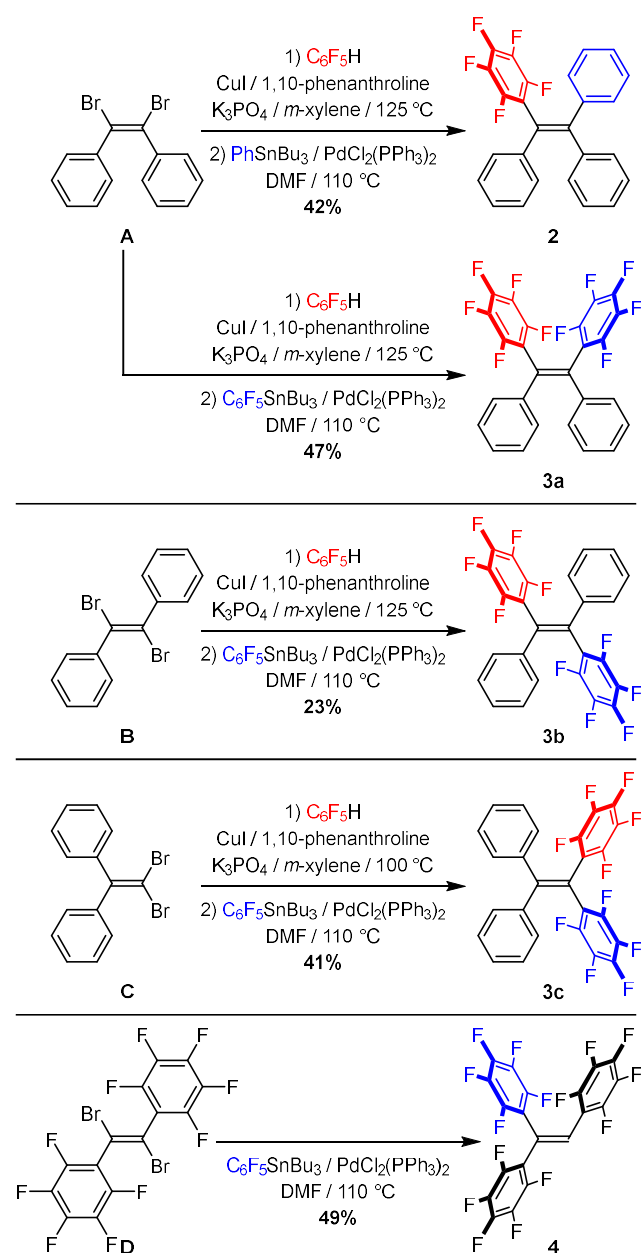


**Figure 1.** Crystal structures of **3a–c** and **4**. Element colors: C—gray, H—white, F—lime. Crystal structure of **3a** is preliminary and shown only to illustrate connectivity; only one of the eight and one of two asymmetric molecules in their unit cells are shown for **3a** and **4**, respectively.

Research on AIE mechanisms suggests that the aggregation of TPE derivatives can restrict the intramolecular rotations,<sup>11a,b</sup> vibrations,<sup>11c</sup> and *Z/E* isomerization along the central C=C bond,<sup>4e,11d-f</sup> which control the molecules' excited state decay via fluorescence. In our case, the mixed H<sub>2</sub>O:THF (99.3:0.7) solvent indeed caused aggregation in all studied compounds, as indicated by the dynamic light scattering profiles which suggested aggregates of average sizes in the 135–165 nm range (Figure S42). Therefore, a nonradiative decay of the excited states of fluorinated TPE derivatives occurred, which cannot be prevented by aggregation.

During our UV/Vis absorption studies, we noticed that fluorinated TPEs are photosensitive in solution (Figure S43): the THF solutions of **2** and **3a** changed color from colorless to yellow upon UV irradiation. Further absorption spectroscopy revealed a new conjugation system with peaks between 302 and 306 nm forming upon irradiation of **2** and **3a–c** (illustrated for **3a** and **3b** in Figure 2; full details in Figure S44). NMR spectroscopy and crystallography

(vide infra and SI) conclusively demonstrated that the UV irradiation at 302 nm of THF solutions of **2** and **3a–c** generated phenanthrenes **5** and **6a–c** (Scheme 2) through either oxidative or redox-neutral photocyclizations. No photocyclization was observed in the case of **4**. Despite extensive experimentation, we were unable to obtain **5** in its pure form. Compounds **1–4** can be seen as derivatives of *cis*-stilbene, which is well-known to photocyclize into *trans*-4a,4b-dihydrophenanthrene under UV irradiation; rapid oxidation of this unstable intermediate produces phenanthrene.<sup>12</sup> The derivatives of *cis*-stilbene with leaving groups (X) such as F,<sup>13a,b</sup> Cl,<sup>13c</sup> Br,<sup>13d</sup> I,<sup>13e</sup> and OCH<sub>3</sub>,<sup>13f</sup> photocyclize into phenanthrenes without an oxidant through the elimination of HX. A few papers also reported that 9,10-diphenylphenanthrenes were detected after the oxidative photocyclization of **1** and its derivatives.<sup>14a–d</sup>

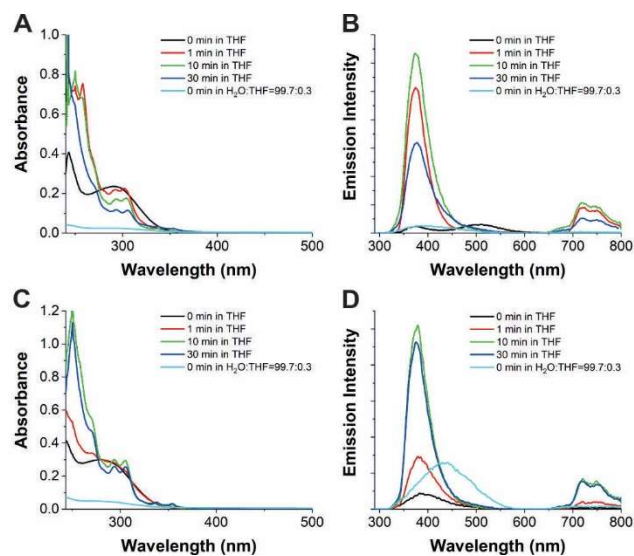


**Figure 1.** Absorption spectra for **3a** (A) and **3b** (C) and emission spectra for **3a** (B,  $\lambda_{exc} = 290$  nm) and **3b** (D,  $\lambda_{exc} = 280$  nm) in 20  $\mu$ M THF solution. The samples were irradiated with UV (302 nm) light for 0, 1, 10, and 30 min. Spectra of **3a** and **3b** in the aggregated state (H<sub>2</sub>O:THF, 99.3:0.7) included for comparison.

Both the *Z*-configured **3a** and its *E*-isomer **3b** generated a mixture of phenanthrenes **6a** and **6b**, suggesting that the rates of *Z/E* photoisomerization and photocyclization are comparable. Since the formation of **6a** requires an oxidant and that of **6b** does not, we tested the effects of oxygen exclusion on the ratio of **6a** and **6b**. The photoreactions of **3a** and **3b** were carried out under either O<sub>2</sub> and N<sub>2</sub> atmosphere, in CH<sub>2</sub>Cl<sub>2</sub> and THF (Table 1). Although all solvents were degassed by the freeze-pump-thaw method, the reactions performed under N<sub>2</sub> atmosphere still generated significant yields of oxidized **6a**. Previous reports suggested that trace amount of O<sub>2</sub> could result in oxidative photocyclization.<sup>12,14b</sup> Reactions run in CH<sub>2</sub>Cl<sub>2</sub> as the solvent gave higher **6a**:**6b** ratios than their counterparts performed in THF; in the case of **3a** as the starting material, **6a** was obtained as essentially the only product. We tentatively attributed this solvent-dependent selectivity to the lower solubility of HF in CH<sub>2</sub>Cl<sub>2</sub> than in THF,<sup>15</sup> which was reported to trap the acid side product in the photocyclization of *cis*-stilbene.<sup>13a,16</sup> Photocyclizations of **2** into **5** and **3c** into **6c** could—and did—only generate one product.

**Scheme 2.** Photocyclization of compounds **2** and **3a–c** into phenanthrenes **5** and **6a–c**. See also Table 1.

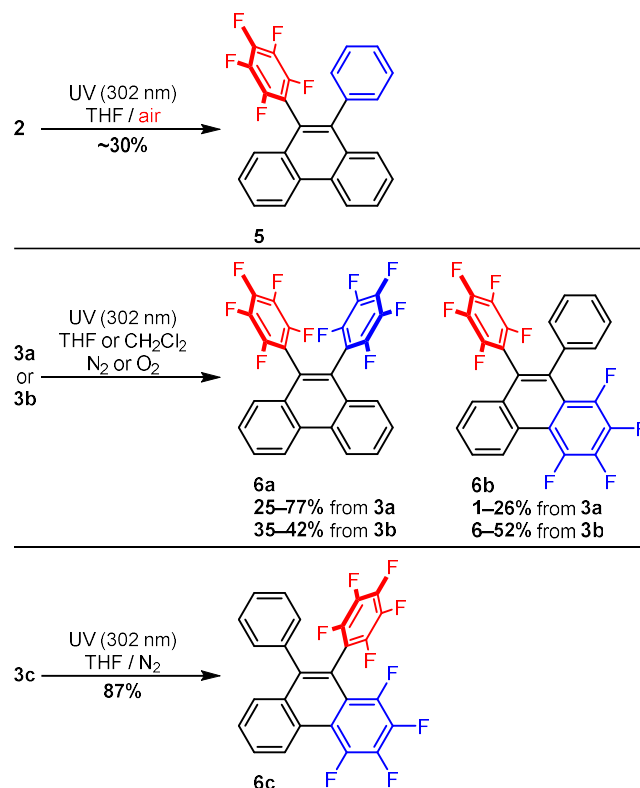


**Table 1.** Photocyclizations of **3a** and **3b** under different conditions.<sup>a</sup>

Reaction	Starting compound	Solvent	Atmosphere	Yield of <b>6a</b>	Yield of <b>6c</b>
1	<b>3a</b>	THF	O <sub>2</sub>	42%	13%
2	<b>3a</b>	THF	N <sub>2</sub>	25%	26%
3	<b>3a</b>	CH <sub>2</sub> Cl <sub>2</sub>	O <sub>2</sub>	73%	1%
4	<b>3a</b>	CH <sub>2</sub> Cl <sub>2</sub>	N <sub>2</sub>	77%	2%
5	<b>3b</b>	THF	O <sub>2</sub>	39%	52%
6	<b>3b</b>	THF	N <sub>2</sub>	36%	34%
7	<b>3b</b>	CH <sub>2</sub> Cl <sub>2</sub>	O <sub>2</sub>	35%	10%
8	<b>3b</b>	CH <sub>2</sub> Cl <sub>2</sub>	N <sub>2</sub>	42%	6%

<sup>a</sup>General reaction conditions: the starting material **3a** or **3b** were dissolved in THF or CH<sub>2</sub>Cl<sub>2</sub> (~2 mg/mL). Then, the solution was degassed by freeze-pump-thaw method and either O<sub>2</sub> or N<sub>2</sub> were bubbled through it. All reactions were carried out at room temperature with UV (302 nm) irradiation for 15 h. Each reaction was repeated three times; the reported yields are averages, determined by <sup>1</sup>H or <sup>19</sup>F NMR with 1,2,4,5-tetrafluorobenzene as the internal standard.

Recent theoretical investigations and ultrafast time-resolved spectroscopy suggested that the cyclization of **1** into 9,10-diphenyl-4a, 4b-dihydrophenanthrene proceeds through a conical intersection, which may be responsible for nonradiative decay.<sup>17</sup> Calculations suggest that **1** cyclizes faster<sup>17a,17c,18</sup> and with less structural reorganization<sup>17a</sup> compared to the rotation along C=C bond during the *Z/E* isomerization. Since the photocyclization of **3a–3c** does not require significant conformational adjustment, their aggregation cannot stop it.<sup>17a</sup> It had been suggested that there is no energy

barrier between the Franck-Condon structure and cyclized structure in the excited state.<sup>17c</sup>

X-ray diffraction quality single crystals of photocyclized **6a** and **6b** were grown from  $\text{CDCl}_3$ , while those of **6c** were obtained from  $\text{CH}_2\text{Cl}_2$ . These crystal structures (Figure 3) reveal remarkably similar  $[\pi\cdots\pi]$  stacking motifs which organize molecules of **6a–c** into dimers with  $[\text{C}\cdots\text{C}]$  interactions of 3.35 Å for **6a**, 3.26–3.37 Å for **6b**, and 3.30 and 3.37 Å for **6c**. Curiously, only the dimer of **6c** organizes its partially fluorinated phenanthrenes in the self-complementary head-to-tail fashion; in **6b**, they stack in an apparently unfavorable head-to-head style. The UV/Vis spectra of **6a–c** are dominated by the absorptions of the phenanthrene moiety at ~300 nm (see Figure S46). These compounds show aggregation-caused quenching (ACQ) because their planarized aromatic structures facilitate  $[\pi\cdots\pi]$  stacking, offering a nonradiative decay pathway (see Table S10 and S11).<sup>1a</sup>

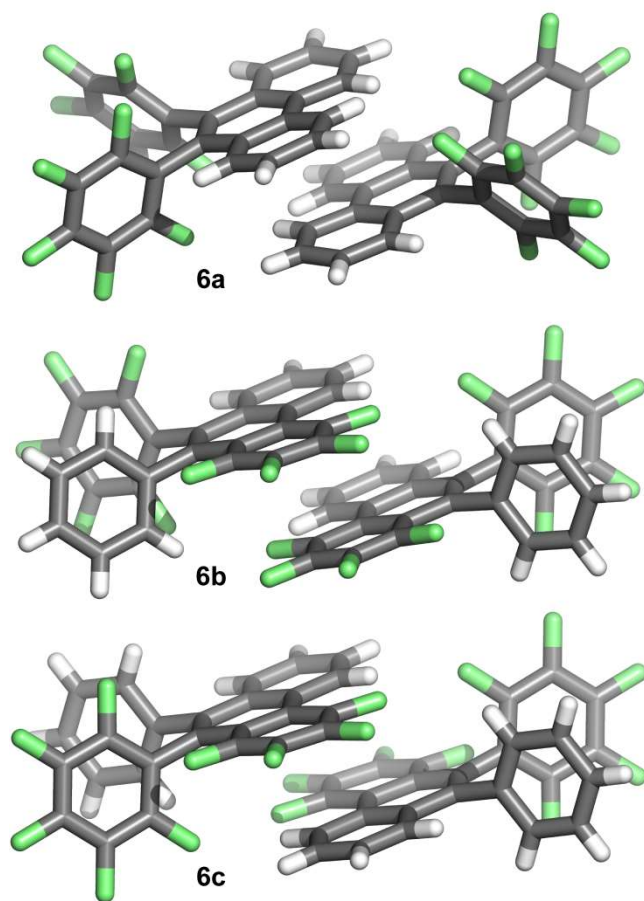


**Figure 3.** Crystal structures of **6a–c**; two molecules are shown to highlight  $[\pi\cdots\pi]$  stacking. Element colors: C—gray, H—white, F—lime.

In conclusion, five TPE derivatives functionalized with pentafluorophenyl groups were synthesized using Pd- and Cu-catalyzed C–C coupling reactions. While fluorescent in the solid state, they do not exhibit aggregation-induced emission, in contrast to the TPE parent system. Instead, their UV irradiation leads to rapid photocyclizations into phenanthrenes. The planarity of these phenanthrenes intensifies their intermolecular interactions, further quenching fluorescence after aggregation. Our results show that the photocyclization in extensively fluorinated TPEs presents an effective

nonradiative decay pathway for their excited states—both in dilute solutions and in the aggregated state.

## ASSOCIATED CONTENT

### Supporting Information

The Supporting Information is available free of charge at [pubs.acs.org](https://pubs.acs.org). Crystallographic Information Files for **3b**, **3c**, **4**, and **6a–c** have been deposited with the Cambridge Crystallographic Data Centre under deposition codes 2082832–2082837.

## AUTHOR INFORMATION

### Corresponding Author

Olafs Daugulis, email: [olafs@uh.edu](mailto:olafs@uh.edu)

Ognjen Š. Miljanić, email: [miljanic@uh.edu](mailto:miljanic@uh.edu)

### Author Contributions

Compounds **2–4** were synthesized by T. L.; Z.Z. prepared compounds **5** and **6**, produced single crystals of **3–4** and **6**, analyzed their optical properties, and performed theoretical calculations. X.W. performed single crystal X-ray diffraction and solution refinement. The manuscript was written by Z.Z. and O.Š.M. incorporating input from all authors.

**The authors declare no competing financial interest.**

## ACKNOWLEDGMENT

We acknowledge the financial support from the National Science Foundation (grant DMR-1904998 to O. Š. M.), the donors of the American Chemical Society Petroleum Research Fund (grant ND-58919 to O. Š. M.), and the Welch Foundation (grant E-1768 to O. Š. M. and chair E-0044 to O. D.). Computational resources were provided by the uHPC cluster, managed by the University of Houston and acquired through the support from the National Science Foundation (MRI-1531814). Prof. Judy I. Wu (UH) is acknowledged for assistance with computations.

## REFERENCES

- (a) Mei, J.; Leung, N. L. C.; Kwok, R. T. K.; Lam, J. W. Y.; Tang, B. Z. Aggregation-Induced Emission: Together We Shine, United We Soar! *Chem. Rev.* **2015**, *115*, 11718. (b) Würthner, F. Aggregation-Induced Emission (AIE): A Historical Perspective. *Angew. Chem. Int. Ed.* **2020**, *59*, 14192. (c) Kokado, K.; Sada, K. Consideration of Molecular Structure in the Excited State to Design New Luminogens with Aggregation-Induced Emission. *Angew. Chem. Int. Ed.* **2019**, *58*, 8632.
- (a) Yang, Z.; Chi, Z.; Mao, Z.; Zhang, Y.; Liu, S.; Zhao, J.; Aldred, M. P.; Chi, Z. Recent Advances in Mechano-Responsive Luminescence of Tetraphenylethylene Derivatives with Aggregation-Induced Emission Properties. *Mater. Chem. Front.* **2018**, *2*, 861–890. (b) Gao, M.; Tang, B. Z. *ACS Sens.* **2017**, *2*, 1382; (c) La, D. D.; Bhosale, S. V.; Jones, L. A.; Bhosale, S. V. Tetraphenylethylene-Based AIE-Active Probes for Sensing Applications. *ACS Appl. Mater. Interfaces* **2018**, *10*, 12189–12216. (d) Cai, X.; Liu, B. Aggregation-Induced Emission: Recent Advances in Materials and Biomedical Applications. *Angew. Chem. Int. Ed.* **2020**, *59*, 9868–9886.
- Zhang, Z.; Miljanić, O. Š. Fluorinated Organic Porous Materials. *Org. Mater.* **2019**, *1*, 19–29.
- (a) Lin, Y.; Chen, G.; Zhao, L.; Yuan, W. Z.; Zhang, Y.; Tang, B. Z. Diethylamino Functionalized Tetraphenylethenes: Structural and Electronic Modulation of Photophysical Properties, Implication for The CIE Mechanism and Application to Cell Imaging. *J. Mater. Chem.*

- C **2015**, 3, 112–120. (b) Xu, P.; Qiu, Q.; Ye, X.; Wei, M.; Xi, W.; Feng, H.; Qian, Z. Halogenated Tetraphenylethene with Enhanced Aggregation-Induced Emission: An Anomalous Anti-Heavy-Atom Effect and Self-Reversible Mechanochromism. *Chem. Commun.* **2019**, 55, 14938–14941. (c) Yang, Z.; Qin, W.; Leung, N. L. C.; Arseneault, M.; Lam, J. W. Y.; Liang, G.; Sung, H. H. Y.; Williams, I. D.; Tang, B. Z. A Mechanistic Study of AIE Processes of TPE Luminogens: Intramolecular Rotation vs. Configurational Isomerization. *J. Mater. Chem. C* **2016**, 4, 99–107. (d) Zhang, H.; Nie, Y.; Miao, J.; Zhang, D.; Li, Y.; Liu, G.; Sun, G.; Jiang, X. Fluorination of the Tetraphenylethene Core: Synthesis, Aggregation-Induced Emission, Reversible Mechano-fluorochromism and Thermofluorochromism of Fluorinated Tetraphenylethene Derivatives. *J. Mater. Chem. C* **2019**, 7, 3306–3314. (e) Kokado, K.; Machida, T.; Iwasa, T.; Taketsugu, T.; Sada, K. Twist of C=C Bond Plays a Crucial Role in the Quenching of AIE-Active Tetraphenylethene Derivatives in Solution. *J. Phys. Chem. C* **2018**, 122, 245–251. (f) Liu, Y.; Zhou, M.; Liu, Y.; Han, X.; Zhang, X.; Liu, S. Host–Guest Interaction-Mediated Fabrication of Aggregation-Induced Emission Supramolecular Hydrogel for Use as Aqueous Light-Harvesting Systems. *Supramol. Chem.* **2020**, 32, 445–451.
5. (a) Chen, T.-H.; Popov, I.; Kaveevivitchai, W.; Chuang, Y.-C.; Chen, Y.-S.; Daugulis, O.; Jacobson, A. J.; Miljanić, O. Š. Thermally Robust and Porous Noncovalent Organic Framework with High Affinity for Fluorocarbons and Freons. *Nat. Commun.* **2014**, 5, doi:10.1038/ncomms6131. (b) Hashim, M. I.; Le, H. T. M.; Chen, T.-H.; Chen, Y.-S.; Daugulis, O.; Hsu, C.-W.; Jacobson, A. J.; Kaveevivitchai, W.; Liang, X.; Makarenko, T.; Miljanić, O. Š.; Popov, I.; Tran, H. V.; Wang, X.; Wu, C.-H.; Wu, J. I. Dissecting Porosity in Molecular Crystals: Influence of Geometry, Hydrogen Bonding, and [ $\pi\cdots\pi$ ] Stacking on the Solid-State Packing of Fluorinated Aromatics. *J. Am. Chem. Soc.* **2018**, 140, 6014–6026.
  6. (a) Zhang, Z.; Hashim, M. I.; Miljanić, O. Š. Aggregation-induced Emission in Precursors to Porous Molecular Crystals. *Chem. Commun.* **2017**, 53, 10022–10025. (b) Zhang, Z.; Hashim, M. I.; Wu, C.-H.; Wu, J. I.; Miljanić, O. Š. Discrimination of Dicarboxylic Acids via Assembly-induced Emission. *Chem. Commun.* **2018**, 54, 11578–11581.
  7. Zhang, Z.; Lieu, T.; Wu, C. H.; Wang, X.; Wu, J. I.; Daugulis, O.; Miljanić, O. Š. Solvation-dependent Switching of Solid-State Luminescence of a Fluorinated Aromatic Tetrapyrrole. *Chem. Commun.* **2019**, 55, 9387–9390.
  8. (a) Yao, M.-L.; Kabalka, G. W.; Blevins, D. W.; Reddy, M. S.; Yong, L. Halodeboronation of Organotrifluoroborates Using Tetrabutylammonium Tribromide or Cesium Triiodide. *Tetrahedron* **2012**, 68, 3738–3743. (b) Organ, M. G.; Ghasemi, H.; Valente, C. The Effect of Vicinyl Olefinic Halogens on Cross-coupling Reactions Using Pd(0) Catalysis. *Tetrahedron* **2004**, 60, 9453–9461. (c) Hau, S. C. K.; Mak, T. C. W. Assembly of Organosilver Coordination Frameworks with Aromatic Ligands Bearing a Terminal Ene-diyne Group. *Polyhedron* **2013**, 64, 63–72. (d) Birchall, J. M.; Bowden, F. L.; Haszeldine, R. N.; Lever, A. B. P. Polyfluoroarenes. Part IX. Decafluorotolan: Synthesis, Properties, and Use as an Organometallic Ligand. *J. Chem. Soc. A* **1967**, 747–753.
  9. Do, H. Q.; Daugulis, O. Copper-Catalyzed Arylation and Alkenylation of Polyfluoroarene C–H Bonds. *J. Am. Chem. Soc.* **2008**, 130, 1128–1129.
  10. Calculation model for **1** was used from the paper published by Jin, Y.; Kim, H.; Kim, J. J.; Heo, N. H.; Shin, J. W.; Teraguchi, M.; Keneko, T.; Aoki, T.; Kwak, G. Asymmetric Restriction of Intramolecular Rotation in Chiral Solvents. *Cryst. Growth Des.* **2016**, 16, 2804–2809.
  11. (a) Shi, J.; Chang, N.; Li, C.; Mei, J.; Deng, C.; Luo, X.; Liu, Z.; Bo, Z.; Dong, Y.; Tang, B. Z. Locking the Phenyl Rings of Tetraphenylethene Step by Step: Understanding The Mechanism of Aggregation-Induced Emission. *Chem. Commun.* **2012**, 48, 10675–10677. (b) Zhang, G.; Chen, Z.; Aldred, M. P.; Hu, Z.; Chen, T.; Huang, Z.; Meng, X.; Zhu, M. Direct Validation of the Restriction of Intramolecular Rotation Hypothesis via the Synthesis of Novel *Ortho*-Methyl Substituted Tetraphenylethenes and Their Application in Cell Imaging. *Chem. Commun.* **2014**, 50, 12058–12060. (c) Leung, N. L. C.; Xie, N.; Yuan, W.; Liu, Y.; Wu, Q.; Peng, Q.; Miao, Q.; Lam, J. W. Y.; Tang, B. Z. Restriction of Intramolecular Motions: The General Mechanism behind Aggregation-Induced Emission. *Chem. Eur. J.* **2014**, 20, 15349–15353. (d) Xiong, J.; Yuan, Y.; Wang, L.; Sun, J.; Qiao, W.; Zhang, H.; Duan, M.; Han, H.; Zhang, S.; Zheng, Y. Evidence for Aggregation-Induced Emission from Free Rotation Restriction of Double Bond at Excited State. *Org. Lett.* **2018**, 20, 373–376. (e) Yang, Z.; Qin, W.; Leung, N. L. C.; Arseneault, M.; Lam, J. W. Y.; Liang, G.; Sung, H. H. Y.; Williams, I. D.; Tang, B. Z. A Mechanistic Study of AIE Processes of TPE Luminogens: Intramolecular Rotation vs. Configurational Isomerization. *J. Mater. Chem. C* **2016**, 4, 99–107. (f) Fang, X.; Zhang, Y.; Chang, K.; Liu, Z.; Su, X.; Chen, H.; Zhang, S. X.; Liu, Y.; Wu, C. Facile Synthesis, Macroscopic Separation, E/Z Isomerization, and Distinct AIE properties of Pure Stereoisomers of an Oxetane-Substituted Tetraphenylethene Luminogen. *Chem. Mater.* **2016**, 28, 6628–6636. (g) Üçüncü, M.; Zeybek, H.; Karakuş, E.; Üçüncü, C.; Emrullahoğlu, M. A New Fluorescent ‘Turn On’ Probe for Rapid Detection of Bi thiols. *Supramol. Chem.* **2020**, 32, 634–641.
  12. Mallory, F. B.; Mallory, C. W. Photocyclization of Stilbenes and Related Molecules. *Org. React.* **1984**, 30, 1.
  13. (a) Li, Z.; Twieg, R. J. Photocyclodehydrofluorination. *Chem. Eur. J.* **2015**, 21, 15534–15539. (b) Geisson, J. K. F.; Kvaran, Á. Photochemical Conversion of 2,6-Dihalo Substituted Methyl  $\alpha$ -Phenylcinnamates. *J. Photochem. Photobiol. A: Chem.* **2001**, 144, 175–177. (c) Cava, M. P.; Mitchell, M. J.; Havlicek, S. C.; Lindert, A.; Spangler, R. Photochemical Routes to Aporphines. New Syntheses of Nuciferine and Glaucine. *J. Org. Chem.* **1970**, 35, 175–179. (d) Olsen, R. J.; Pruet, S. R. Photocyclization of *o*-Halostilbenes. *J. Org. Chem.* **1985**, 50, 5457–5460. (e) Kupchan, S. M.; Wormser, H. C. Tumor Inhibitors. X.1 Photochemical Synthesis of Phenanthrenes. Synthesis of Aristolochic Acid and Related Compounds. *J. Org. Chem.* **1965**, 30, 3792–3800. (f) Mallory, F. B.; Rudolph, M. J.; Oh, S. M. Photochemistry of Stilbenes. 8. Eliminative Photocyclization of *o*-Methoxystilbenes. *J. Org. Chem.* **1989**, 54, 4619–4626.
  14. (a) Collins, D. J.; Hobbs, J. J. The Influence of Copper Halides on the Course of Photolysis of  $\alpha,\alpha'$ -Disubstituted Stilbenes. *Aust. J. Chem.* **1967**, 20, 1905–1920. (b) Bunker, C. E.; Hamilton, N. B.; Sun, Y. Quantitative Application of Principal Component Analysis and Self-Modeling Spectral Resolution to Product Analysis of Tetraphenylethylene Photochemical Reactions. *Anal. Chem.* **1993**, 65, 3460–3465. (c) Huang, G.; Ma, B.; Chen, J.; Peng, Q.; Zhang, G.; Fan, Q.; Zhang, D. Dendron-Containing Tetraphenylethylene Compounds: Dependence of Fluorescence and Photocyclization Reactivity on the Dendron Generation. *Chem. Eur. J.* **2012**, 18, 3886–3892. (d) Aldred, M. P.; Li, C.; Zhu, M. Optical Properties and Photo-oxidation of Tetraphenylethene-Based Fluorophores. *Chem. Eur. J.* **2012**, 18, 16037–16045.
  15. [http://periodic-table-of-elements.org/SOLUBILITY/hydrogen\\_fluoride](http://periodic-table-of-elements.org/SOLUBILITY/hydrogen_fluoride). Last accessed on May 6, 2021.
  16. Talele, H. R.; Gohil, M. J.; Bedekar, A. V. Synthesis of Derivatives of Phenanthrene and Helicene by Improved Procedures of Photocyclization of Stilbenes. *Bull. Chem. Soc. Jpn.* **2009**, 82, 1182–1186.
  17. (a) Guan, J.; Wei, R.; Prlj, A.; Peng, J.; Lin, K.; Liu, J.; Han, H.; Corminboeuf, C.; Zhao, D.; Yu, Z.; Zheng, J. Direct Observation of Aggregation-Induced Emission Mechanism. *Angew. Chem. Int. Ed.* **2020**, 59, 14903–14909. (b) Cai, Y.; Du, L.; Samedov, K.; Gu, X.; Qi, F.; Sung, H. H. Y.; Patrick, B. O.; Yan, Z.; Jiang, X.; Zhang, H.; Lam, J. W. Y.; Williams, I. D.; Phillips, D. L.; Qin, A.; Tang, B. Z. Deciphering the Working Mechanism of Aggregation-Induced Emission of Tetraphenylethylene Derivatives by Ultrafast Spectroscopy. *Chem. Sci.*

- 2018**, *9*, 4662–4670. (c) Gao, Y.; Chang, X.; Liu, X.; Li, Q.; Cui, G.; Thiel, W. Excited-State Decay Paths in Tetraphenylethene Derivatives. *J. Phys. Chem. A* **2017**, *121*, 2572–2579.
18. (a) Prlj, A.; Došlić, N.; Corminboeuf, C. How Does Tetraphenylethylene Relax from Its Excited States? *Phys. Chem. Chem. Phys.* **2016**, *18*, 11606–11609. (b) Tran, T.; Prlj, A.; Lin, K.; Hollas, D.; Corminboeuf, C. Mechanisms of Fluorescence Quenching in Prototypical Aggregation-Induced Emission Systems: Excited State Dynamics with TD-DFTB. *Phys. Chem. Chem. Phys.* **2019**, *21*, 9026–9035.
-